Modulation of WN_x/Ge Schottky barrier height by varying N composition of tungsten nitride*

Wei Jiang-Bin(魏江镔)[a], Chi Xiao-Wei(池晓伟)[a], Lu Chao(陆 超)[a], Wang Chen(王 尘)[a], Lin Guang-Yang(林光杨)[a], Wu Huan-Da(吴焕达)[a], Huang Wei(黄 巍)[a]†, Li Cheng(李 成)[a]‡, Chen Song-Yan(陈松岩)[a], and Liu Chun-Li(刘春莉)[b]

[a] *Department of Physics, Semiconductor Photonics Research Center, Xiamen University, Xiamen* 361005, *China*
[b] *Department of Physics, Hankuk University of Foreign Studies, Yongin* 449-791, *Korea*

(Received 22 December 2014; revised manuscript received 2 February 2015; published online 18 May 2015)

Modulation of the Schottky barrier heights was successfully demonstrated for WN_x/p-Ge and WN_x/n-Ge contacts by increasing the nitrogen component in the WN_x films. The $WN_{0.38}$/p-Ge contact exhibits rectifying characteristic and an apparent Schottky barrier of 0.49 eV while the $WN_{0.38}$/n-Ge Schottky contact exhibits quasi-Ohmic current–voltage characteristics. Dipoles formed at the contact interface by the difference of the Pauling electronegativities of Ge and N are confirmed to alleviate the Fermi-level pinning effect.

Keywords: germanium, Fermi-level pinning, Schottky barrier height modulation, tungsten nitride

PACS: 73.40.Sx, 73.40.Ei, 73.61.At **DOI:** 10.1088/1674-1056/24/7/077306

1. Introduction

Germanium (Ge) is considered to be a good candidate material due to its high carrier mobilities and large optical absorption coefficient at the wavelength for optical communication in electronic and photonic device applications. Although a high performance p-type Ge channel metal–oxide–semiconductor field-effect transistor (MOSFET) has been demonstrated,[1] the n-type Ge channel MOSFET still suffers from two serious challenges: (a) low electrical activation of donor impurities and fast diffusion of n-Ge dopant that hinder fabricating low resistivity, shallow source/drain junctions.[2] (b) strong Fermi-level pinning effect on Ge in the vicinity of the valence band maximum of Ge results in a high effective electron Schottky barrier height (SBH) when metals contact with n-Ge. The high SBH results in high series contact resistivity[3] while Ohmic contact with p-Ge is normally achieved.

To control the SBHs of the metal/Ge contact, several methods have been proposed to alleviate the FLP effect. One is inserting an ultrathin insulating interfacial layer (e.g., TiO_2,[4] Al_2O_3,[5] GeO_x,[6] Si_3N_4,[7] a-Ge[8]). Segregation of addictive elements (such as S,[9] Se,[10] P,[11]) at the metal/Ge interface is another. Recently, metallic nitrides such as TiN[12] and TaN[13] have been confirmed to form Ohmic contact to n-type Ge intrinsically. In this work we study the SBHs of the WN_x film on both n-type and p-type Ge (100) substrates with various N compositions. Typical electrical rectifying characteristics of the WN_x/p-Ge contact and Ohmic contact of WN_x/n-Ge are obtained.

2. Experimental procedure

P-type and n-type Ge (100) substrates with a resistivity of 0.1 Ω·cm were used for schottky diodes fabrication. All of the Ge wafers were firstly circularly degreased in an ultrasonic bath of acetone and ethanol, and then immersed in hydrofluoric acid solution ($HF:H_2O$ = 1:50) to remove the native oxide, rinsed with deionized water, and finally blown dry by nitrogen. The diode areas were defined by conventional lithography. Then WN_x thin films were deposited on these substrates by reactive sputtering in a magnetron sputtering system (JC-500-3/D D.C.) with mixed N_2–Ar gas atmosphere for 30 min. The base vacuum pressure of the sputtering system was 1.0×10^{-3} Pa. Tungsten with a purity of 99.99% was used as the target. During sputtering, the Ar gas flow was fixed at 50 sccm while the N_2 gas flow was changed from 0 sccm to 35 sccm. For the electrical measurement, WN_x/Ge contacts with a diameter of 120 μm were formed by a lift-off process and a 300-nm Al layer was sputtered on the backside of the wafers to form the Ohmic contact. The samples were analyzed by four point probes, x-ray diffraction (XRD), x-ray photoelectron spectroscopy (XPS), and *I*–*V* characteristics.

3. Results and discussion

Because the growth rates under different N_2 flow rates are all about 4 nm/min, the thicknesses of the obtained WN_x films with different N_2 flow rates are all around 120 nm. Sheet resistances of the WN_x films with different N_2 flow rates are

*Project supported by the National Natural Science Foundation of China (Grant Nos. 61176092 and 61474094), the National Basic Research Program of China (Grant Nos. 2012CB933503 and 2013CB632103), and the National Natural Science Foundation of China–National Research Foundation of Korea Joint Research Project (Grant No. 11311140251).

†Corresponding author. E-mail: weihuang@xmu.edu.cn
‡Corresponding author. E-mail: lich@xmu.edu.cn

© 2015 Chinese Physical Society and IOP Publishing Ltd

shown in Fig. 1. For pure W film, the resistivity is calculated to be about 120 μΩ·cm, which is higher than the resistivity data for bulk W (∼ 5.5 μΩ·cm) because of surface/grain boundary scattering. When the N_2 flow rates increase, sheet resistance of the WN_x film become even higher than that of pure W. However, when the N_2 flow rate is above 25 sccm, the sheet resistance of WN_x tends to be stable at about 34 Ω/□. The increase of the film resistivity was ascribed to the increasing inclusion of nitrogen atoms in the WN_x crystal lattice which can bring appreciable band structure changes and a decreasing carrier density.

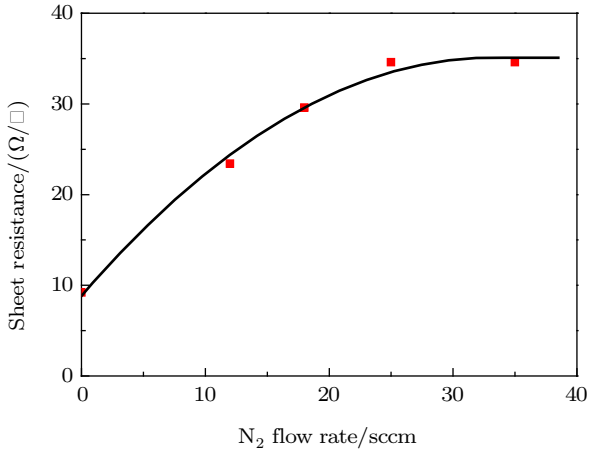


Fig. 1. (color online) Sheet resistance of the WN_x film fabricated with various rates of N_2 flow from 0 sccm to 35 sccm.

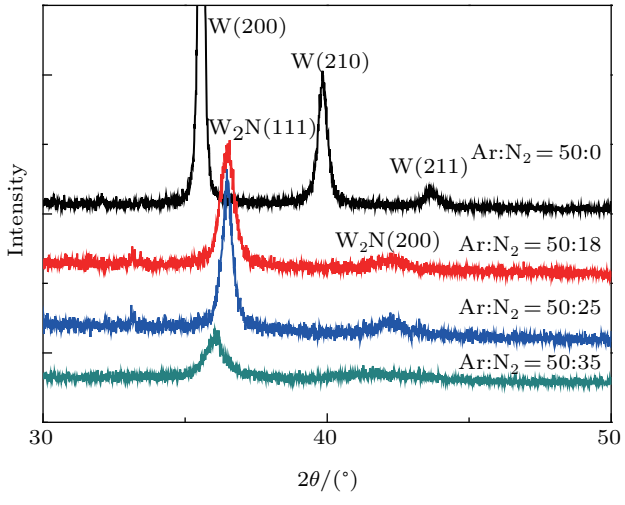


Fig. 2. (color online) θ–2θ XRD scan of the WN_x film formed at different N_2 flow rates from 0 to 35 sccm.

XRD is used to identify the crystalline phases of the samples. Figure 2 shows the XRD patterns of the WN_x films with different N compositions. The W(200), W(210), and W(211) diffraction peaks are clearly observed for the W deposited in pure Ar atmosphere. When the N_2 flow reaches 18 sccm, the crystalline phase is identified as W_2N and all the films show a preferred orientation of (111). However, the peak positions are a little lower than the standard value of 37.73° for W_2N(111) in the ICDD cards.[14] A continuous left shift of the W_2N(111) x-ray diffraction peak with further increasing of the N_2 flow, is found to be consistent with the gernerally reported data. This has been explained by the existence of nitrogen excess in the interstitial positions of the W_2N lattice and the expansion of the W_2N lattice.[15]

In order to evaluate the nitrogen component of the WN_x films, the deconvoluted W 4f XPS spectrum is depicted in Fig. 3. The W 4f spectrum pertained to W–N and W–O bonds and there is no obvious W–W bonds. The W–O bond was caused by residual oxygen in the deposition chamber. The simulated W 4f 7/2–W 4f 5/2 peaks located at 31.6 eV and 33.7 eV shall pertain to the W_2N phase (W–N bond).[16] In addition, the 397.5–397.6 eV binding energy of N 1s electrons was close to the reported value for W_2N (397.3 eV). By integrating the XPS peaks' area, the nitrogen component x of these samples was determined to be $x = 0.28$, 0.32, and 0.37. Both XRD and XPS measurements indicate that the nitrogen components increase as the N_2 flow rate increases.

Figure 4 shows the current density–voltage (J–V) characteristics measured at room temperature for WN_x/p-Ge and WN_x/n-Ge contacts prepared under two different compositions of W nitride. The J–V curve of the W/Ge contact is also shown for comparison. The thermionic emission model is used to extract the SBH of the samples with rectification characteristics. The relationship between current (I) and voltage (V) used for the calculations is expressed as

$$I = I_s \left[\exp \frac{q(V - IR_s)}{nk_BT} - 1\right],$$

$$I_s = AA^*T^2 \exp\left(-\frac{\Phi_B}{k_BT}\right),$$

where I_s is the reverse saturation current, A^* is the Richardson constant ($A^* = 143$ A·cm^{-2}·K^{-2} for n-Ge and $A^* = 43$ A·cm^{-2}·K^{-2} for p-Ge), k_B is the Boltzman constant, $A = 2.01 \times 10^{-4}$ cm^{-2} is the diode area, Φ_B is the SBH, n is the ideality factor, q is the electron's charge, V is the applied bias, and R_s is the series resistance. The SBHs extracted from the J–V curves of the WN_x/Ge contact are shown in Table 1.

Typical rectifying characteristics are observed for the Schottky W/n-Ge contact. With the increase of the N composition in the W nitride, the reverse saturation current density of WN_x/n-Ge increases while the forward current density of WN_x/p-Ge decreases. The electrical property of WN_x/n-Ge gradually changes from rectification of 0.50 eV to Ohmic while that of WN_x/p-Ge changes from Ohmic to rectification of 0.49 eV. A rectification ratio of nearly 10^3 for WN_x/p-Ge is obtained as the N_2 flow rate reaches 35 sccm. As is well known, Ohmic characteristics for p-Ge were experimentally

observed irrespective of the metal vacuum work-function because the Fermi-levels at metal/Ge interfaces are pinned near the valence band edge of Ge. However, the significant SBH modulation of WN_x/p-Ge is observed in the experiment, illustrating that some mechanisms act on the WN_x/p-Ge contact and realize the Femi level depinning effect.

There are several mechanisms to explain the SBH modulation of the metal-semiconductor contact. One widely recognized mechanism is to minimize metal-induced gap states (MIGS)[17,18] by inserting an interfacial insulating layer which blocks the electron wave function penetrating from the metal into the semiconductor. Other authors have argued that the interface defects caused by ion implantation or dipoles at the metal-semiconductor interface at the metal-semiconductor interface will also alter the effective SBH. In the case of WN_x/Ge contact, MIGS is obviously not applicable to explain the SBH modulation effect because the metallic WN_x film does not block penetrating the electron wave. If we consider the

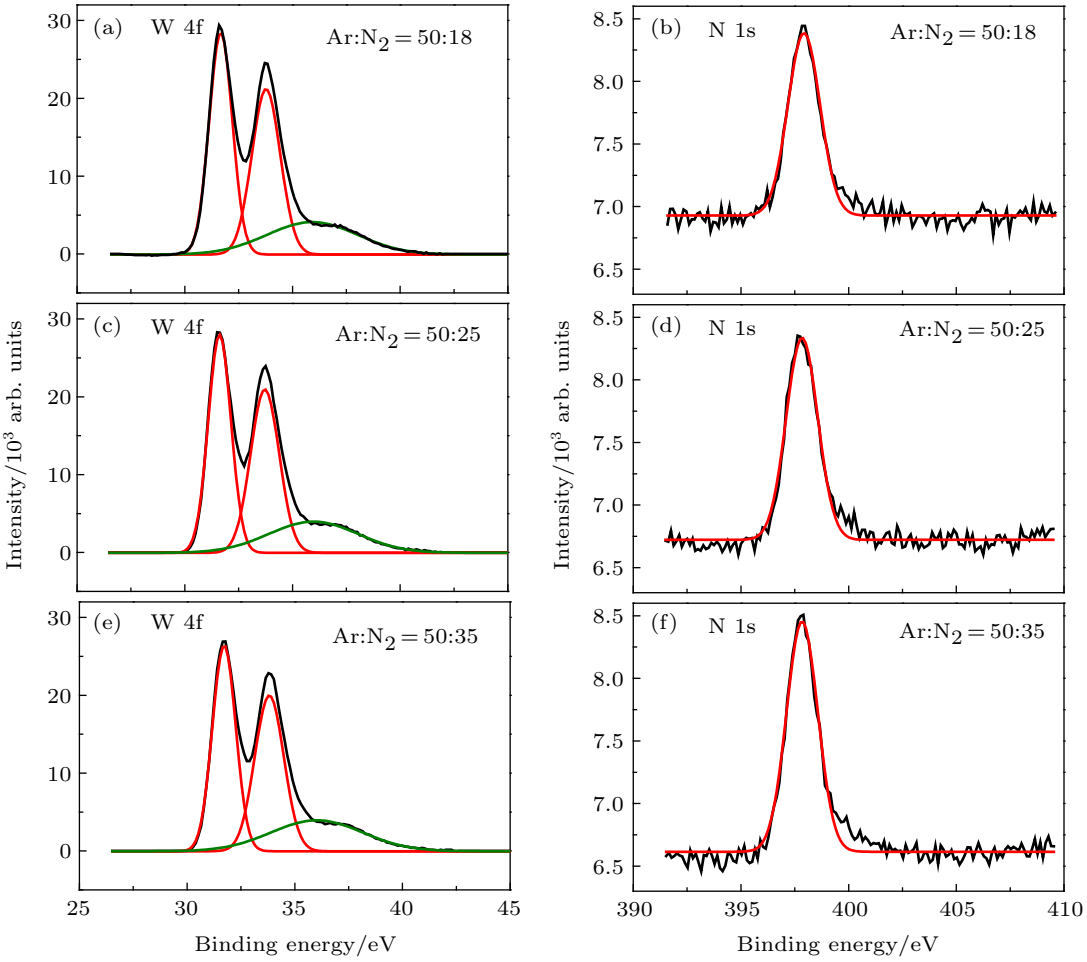


Fig. 3. (color online) XPS spectra of W 4f and N 1s for the WN_x films prepared with different Ar/N_2 flow rates. (a) W 4f, $Ar : N_2 = 50 : 18$, (b) N 1s, $Ar : N_2 = 50 : 18$, (c) W 4f, $Ar : N_2 = 50 : 25$, (d) N 1s, $Ar : N_2 = 50 : 25$, (e) W 4f, $Ar : N_2 = 50 : 35$, (f) N 1s, $Ar : N_2 = 50 : 35$.

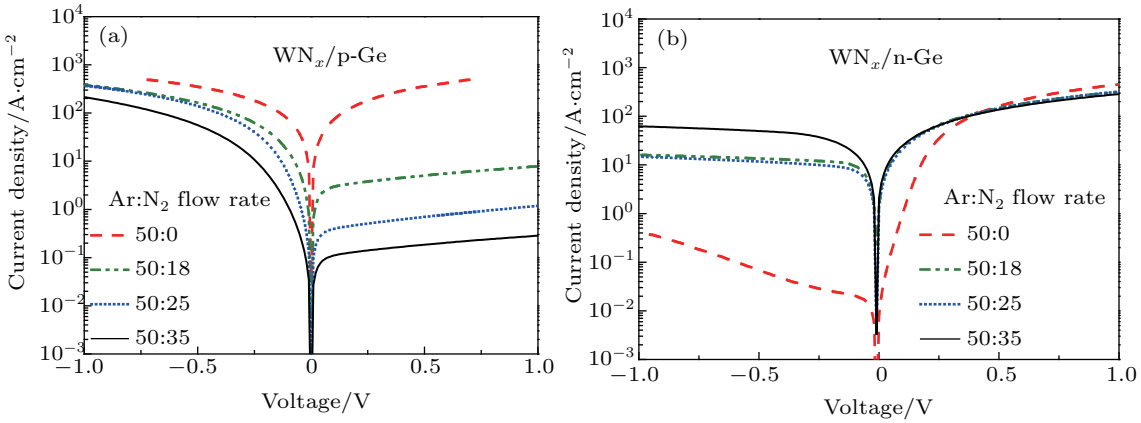


Fig. 4. (color online) *J–V* characteristics of the WN_x/Ge films formed with different Ar/N_2 flow rate ratios. (a) WN_x/p-Ge (b) WN_x/n-Ge.

Table 1. The extracted SBHs of different samples and their rectification ratios under ±1.0 V bias. "(O)" denotes Ohmic or quasi-Ohmic contact.

Type of Ge	N_2 flow rate/sccm	Rectification ratio @−1 V/1 V	Ideality factor	SBH/eV
n-type	0	1159	1.28	0.50
	18	31	1.15	0.37
	25	33	1.37	0.37
	35	13	–	(O)
p-type	0	1	–	(O)
	18	49	1.72	0.37
	25	314	1.81	0.42
	35	765	1.76	0.49

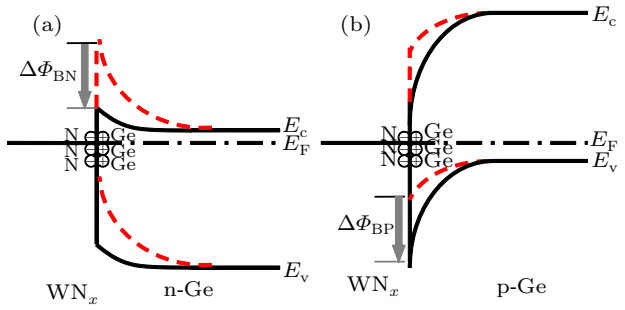


Fig. 5. (color online) Schematic band diagram of the pinning-alleviated WN_x/n-Ge (a) and WN_x/p-Ge (b) contacts by the interfacial dipoles layer. Here, E_c is the conduction band edge, E_v is the valence band edge, and E_F is the Fermi level.

interface defect mechanism, the obtained low effective SBH is formed by the current leakage through the interface defects. Such a leakage is natural regardless on the conduction type of the contact semiconductor, and the low rectification ratios or Ohmic behavior should be observed on both metal/n-Ge and metal/p-Ge contacts. However, in our WN_x/p-Ge contact sample, the rectifying characteristics are clearly observed. This result explicitly excluded the possibility of interface leakage by defects, but further illustrated the validity of the dipoles layer model which was recently reported by Wu *et al.*[19] One may further argue that the different work functions of WN_x could be the reason of SBH changing. According to the previous report written by Jiang (Ref. [16]), the work functions range from 4.39 eV to 5.01 eV for WN_x with various N contents compared to 4.67 eV for pure W. However, those work functions are not monotonous as the N content increases. It is also difficult to conclude any correlation between the work function of WN_x and the SBH evolution even if the surface Fermi-level pinning effect is ignored.

According to the dipoles layer model, the N and W atoms formed bonds with Ge at the WN_x/Ge contact interface. However, the N–Ge bond is not pure covalent but partially ionic because the Pauling electronegativities of Ge (2.01) and N (3.04) are largely discrepant, so many N–Ge bonds can be dealt with as interfacial dipoles (see Fig. 5). The potential drop arose from the interfacial dipoles strongly affecting the energy band bending and modulating the WN_x/Ge contact SBH. From our experiment results shown in Table 1, it is clearly observed that the SBH modulation tendency of the WN_x/p-Ge is just contrary to that of the WN_x/n-Ge, just providing a direct evidence of the dipoles layer model which was established for WN_x/Ge contact.

4. Conclusions

In summary, thin WN_x films have been fabricated by reactive magnetron sputtering of tungsten in an Ar–N_2 gas mixture of different flow rates. As the N_2 flow rates increase, the nitrogen components increase from 0 to 0.38. By increasing the nitrogen components of the WN_x film, the contact properties have been drastically changed from Schottky to Ohmic for n-Ge and from Ohmic to Schottky characteristics for p-Ge, respectively. The SBH of WN_x/n-Ge gradually changes from 0.50 eV to a value smaller than 0.30 eV while the SBH of WN_x/p-Ge changes from a value smaller than 0.30 eV to 0.49 eV. This experimental fact strongly suggests that the dipoles layer model is the dominant SBH mechanism in the WN_x/Ge contact.

References

[1] Hashemi P, Chern W, Lee H S, Teherani J T, Zhu Y, Gonsalvez J, Shahidi G G and Hoyt J L 2012 *IEEE Electron Device Lett.* **33** 943
[2] Koike M, Kamata Y, Ino T, Hagishima D, Tatsumura K, Koyama M and Nishiyama A 2008 *J. Appl. Phys.* **104** 023523
[3] Dimoulas A, Tsipas P, Sotiropoulos A and Evangelou E K 2006 *Appl. Phys. Lett.* **89** 252110
[4] Lin J Y J, Roy A M, Nainani A, Sun Y and Saraswat K C 2011 *Appl. Phys. Lett.* **98** 092113
[5] Gajula D R, Baine P, Modreanu M, Hurley P K, Armstrong B M and McNeill D M 2014 *Appl. Phys. Lett.* **104** 012102
[6] Nishimura T, Kita K and Toriumi A 2008 *Appl. Phys. Express* **1** 051406
[7] Kobayashi M, Kinoshita A, Saraswat K, Wong H S P and Nishi Y 2009 *J. Appl. Phys.* **105** 023702
[8] Liu H H, Wang P, Qi D F, Li X, Han X, Wang C, Chen S Y, Li C and Huang W 2014 *Appl. Phys. Lett.* **105** 192103
[9] Ikeda K, Yamashita Y, Sugiyama N, Taoka N and Takagi S I 2006 *Appl. Phys. Lett.* **88** 152115
[10] Tong Y, Liu B, Lim P S Y and Yeo Y C 2012 *Electron Dev. Lett.* **33** 773
[11] Koike M, Kamimuta Y and Tezuka T 2011 *Appl. Phys. Express* **4** 021301
[12] Wu H D, Huang W, Lu W F, Tang R F, Li C, Lai H K, Chen S Y and Xue C L 2013 *Appl. Surf. Sci.* **284** 877
[13] Wu Z, Huang W, Li C, Lai H K and Chen S Y 2012 *IEEE Trans. Electron Dev.* **59** 1328
[14] ICDD card No. 025-1257
[15] Addonizio M L, Castaldo A, Antonaia A, Gambale E and Iemmo L 2012 *J. Vac. Sci. Technol. A* **30** 031506
[16] Jiang P C, Lai Y S and Chen J S 2006 *Appl. Phys. Lett.* **89** 122107
[17] Nishimura T, Kita K and Toriumi A 2007 *Appl. Phys. Lett.* **91** 123123
[18] Zhou Y, Han W, Wang Y, Xiu F, Zou J, Kawakami R and Wang K 2010 *Appl. Phys. Lett.* **96** 102103
[19] Wu H D, Wang C, Wei J B, Huang W, Li C, Lai H K, Li J, Liu C L and Chen S Y 2014 *IEEE Electron Device Lett.* **35** 1188